Compact Eye-Safe LIDAR Source for Airborne Laser Scanning – The CALIBER Project

COMPACT EYE-SAFE LIDAR SOURCE FOR AIRBORNE LASER SCANNING - THE CALIBER PROJECT

NADIA G. BOETTI[1*], AMIEL ISHAAYA[2], MIRCEA GUINA[3], DAVIDE JANNER[4], DANIEL MILANESE[5], DIEGO PUGLIESE[4], ANTTI PENTTINEN[3], ANTTI HÄRKÖNEN[3], OMRI MOSCHOVITS[2], YAIR ALON[2], FEDERICO LEONE[1]

1 - LINKS Foundation – Leading Innovation and Knowledge for Society, Via P. C. Boggio 61, 10138 Torino, Italy

2 - Ben-Gurion University of Negev, School of Electrical and Computer Engineering, 8410501 Beer-Sheva, Israel

3 - Tampere University, Optoelectronics Research Centre, Korkeakoulunkatu 3, 33720 Tampere, Finland

4 - Politecnico di Torino – DISAT and RU INSTM, Corso Duca degli Abruzzi 24, 10129 Torino, Italy

5 - Università di Parma – DIA and RU INSTM, Parco Area delle Scienze 181/A, 43124 Parma, Italy

*To whom correspondence should be addressed.

Abstract- A high power, ultra-compact, lightweight, and low cost eye-safe laser source for a Light Detection and Ranging (LIDAR) system is currently under development in the framework of the NATO Science for Peace and Security project "CALIBER", with the aim to be installed on small Unmanned Aerial Vehicles (UAVs) for surveillance of borders and sensitive areas, with saving in manpower and equipment.

Keywords: LIDAR, phosphate glass, microchip laser, glass amplifier, optical fiber

1. Introduction

The security and protection of borders, sensitive infrastructures and strategic sites, such as overseas gas and oil extraction platforms, maritime infrastructures and power plants, is of paramount importance. This capability is directly related to current and future security problems of NATO countries, allowing for early hazard detection, protection of strategic infrastructures, and the general securing of Europe's borders (land and sea) (https://www.nato.int/cps/en/natohq/85291.htm).

Current monitoring is mainly done by human patrols securing the perimeter or border, in combination with Charge-Coupled Device (CCD) cameras and various night vision sensors positioned statically in overlooking locations, or on UAVs when a more complete overview of the installments and of the surroundings is needed. The current monitoring methods are limited in terms of continuous coverage and resolution, pose threats to the security forces, and involve high cost (work force and equipment).

Book Title Information

Compared to other sensors, LIDAR systems have proved to be more effective and precise for remote sensing applications, ranging from the detection of obstacles for automobiles and aircrafts, to the topographic investigation of landscapes, and to the detection of wind turbulence and hazardous gases or pollutants (Overton, 2017; Schmitt, 2017; Pulikkaseril and Lam, 2019; Chen et al., 2019). Their significant advantage over standard CCD or night vision cameras consists in the ability to measure distances with high accuracy and build a three-dimensional (3D) map of the scanned area.

A LIDAR system includes a laser source or transmitter, optics for precise laser scanning, a sensitive photodetector or receiver and synchronization and data processing electronics (https://esto.nasa.gov/files/Lidar_TechStrategy_%202016.pdf).

The light emitter is a key element of the system and contributes to the overall system performance. The quality of the sensing strongly depends on the type of source employed, in terms of wavelength, pulse width, average and peak power, which altogether define the precision and reliability of the overall system.

However, high-power eye-safe LIDAR sources that have been used for decades are bulky, heavy, and expensive, which does not make them suitable for installation on small/medium UAVs. For example, the early eye-safe time-of-flight (TOF) LIDAR systems exploited low repetition rate, ns-pulsed, high energy (10's of mJ's) solid state lasers, typically based on Er:glass or Nd:YAG, with an Optical Parametric Oscillator (OPO) wavelength converter operating at 1.5 μm wavelength (Spinhirne et al., 1995).

With the recent development of 1.5 μm Er:glass fiber lasers, LIDAR sources became smaller and more lightweight. Here, instead of low repetition rate and high energy pulses, high repetition rates (10-100 kHz) and low energy pulses are used. These lasers are typically built with multiple amplification stages, resulting in high pricing, and can be packed in relatively small size modules.

A flexible and advantageous approach to realize a high-power LIDAR source is the Master Oscillator Power Amplifier (MOPA) configuration. A seed laser with high spectral quality is followed by a single- or multi-stage power amplifier that boosts the output power to attain the needed energy.

The NATO Science for Peace and Security project "CALIBER" (CompAct eye-safe Lidar source for AirBorne lasER scanning) aims to develop a compact, lightweight and low-cost version of a LIDAR source, by integrating a Semiconductor Saturable Absorber Mirror (SESAM) Q-switched microchip seed laser and a new Er:Yb power amplifier in a compact MOPA configuration, which combines high repetition rate and high peak power at the "eye-safe" wavelength of 1535 nm.

In this work we report on the development until now of the key components of the CALIBER laser source, i.e. the seed laser and the power amplifier, as well as the preliminary work towards their integration into a LIDAR source. This source will then be inserted into a LIDAR laboratory system for a range finding proof of concept.

2. The microchip seed laser

Pulsed Q-switched microchip lasers (Zayhowski, 2013; Häring et al., 2001; Gorbachenya et al., 2015) are highly compact and rugged laser sources, capable of producing energetic pulses with multi-kW peak power. Q-switched microchip lasers consist of a thin piece of laser gain material (crystal or glass), which is optically contacted to a saturable absorber that is used for initiating the pulsed operation. The saturable absorber can be made of doped glass, crystal, or semiconductor material. The gain element and the saturable absorber will form a monolithic structure, with plane-plane cavity geometry. The necessary laser mirrors are deposited directly on the cavity surfaces, making the laser free of cavity alignment. A laser operation in plane-plane type resonator is typically stabilized by a thermal lens. The laser output parameters, such as pulse width, pulse energy, pulse repetition rate, and spectrum are dependent on the combination of the gain material, saturable absorber, mode diameter, and the laser coatings.

Within the CALIBER project, Erbium-doped phosphate glass gain material (λ = 1535 nm), 976 nm diode pumping and SESAMs were used. The SESAMs consist of a Distributed Bragg Reflector (DBR) and a Quantum Well (QW)-based absorber section, fabricated on a InP substrate in single step by solid-source Molecular Beam Epitaxy (MBE). In comparison to doped glass/crystal-based absorbers, the SESAMs exhibit certain unique properties: 1) the absorber layers are very thin (only a few micrometers thick), which helps to shorten the laser cavity and consequently the laser pulses; 2) the optical properties of the SESAMs can be tailored by the composition and design of the quantum wells, which makes this approach very flexible and allows customization. The semiconductor fabrication methods also allow high volume and low unit-cost production when necessary.

In CALIBER, 20–100 kHz pulse repetition rate and 1–2 ns pulse duration with 1 kW peak power were targeted. This combination of parameters was chosen to provide sufficient speed of measurements and suitable measurement accuracy and distance. In total, over 100 individual samples with different SESAMs, gain elements and coatings were tested. The laser output parameters obtained for different sample combinations are

summarized in Table 1. A typical laser spectrum and light output / repetition rate curves are presented in Figs. 1a and 1b, respectively.

Table 1. Laser output parameters tested in CALIBER.

	Repetition rate (kHz)	Peak power (kW)	Average power (mW)	Pulse width (ns)
Target parameters	20-100	1.0	10	1.0
	20	1.6	55	1.6
Measured results	50	1.0	63	1.2
	100	0.3	73	2.6

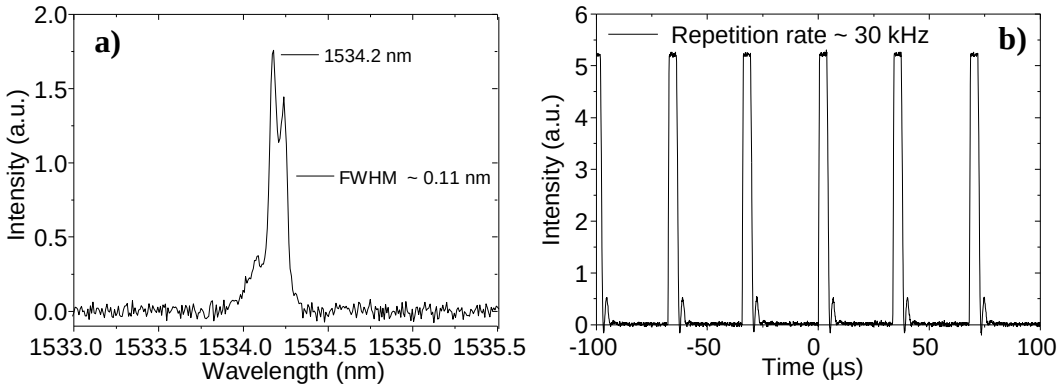

Figure 1. a) Typical laser spectrum and b) light output / repetition rate curves. Repetition rate was measured with a slow photodiode, PDA50B-EC, and therefore not showing the correct pulse width.

The obtained results demonstrate that using SESAM technology it is possible to tailor the output parameters in a wide range, by customizing the SESAM and coating designs. A lifetime test was also carried out at 30 kHz, 2.5 ns, and 500 W peak power, showing no signs of performance drop in 1800 h of operation. Based on these observations we believe that SESAM-based Q-switched microchip lasers are well suited for drone/UAV-based LIDAR systems requiring higher performance than common diode-based systems.

3. The waveguide amplifier

Following the CALIBER project requests of a high degree of compactness while retaining high performance and low cost, the choice for the optical amplifier fell on an Yb/Er co-doped phosphate glass-based waveguide. The use of a glass material shows the advantage, over the other types of materials, of combining: chemical stability, excellent homogeneity, good thermo-mechanical properties and a viscosity–temperature relationship that allows for shaping the waveguide into the form of optical fibers or rods. Moreover, glass displays a wide flexibility of the chemical composition and doping, allowing the preparation of multi-component glasses with properties that can be customized to meet the needs of the different applications (Yamane and Asahara, 2004).

Among the other oxide glass systems, multi-component phosphate glasses are recognized to be an ideal host material for engineering the amplification stage of a pulsed MOPA as they can be doped with a large amount of Rare-Earth (RE) ions (up to 10^{21} ions/cm^3) without clustering thanks to the presence of phosphorus, which introduces non-bridging oxygens in the structure (Boetti et al., 2017; Lee et al., 2006). This enables the realization of an active medium with high optical gain in short length (> 5 dB/cm) and thus mitigating nonlinear optical effects. Moreover, this glass system possesses a large glass formation region, good thermo-mechanical and chemical properties, high emission cross-sections, low nonlinear refractive index, and no evidence of photodarkening even at high population inversion (Jiang et al., 2003; Boetti et al., 2015; Qiu et al., 2004).

A highly stable and robust glass host, suitable for the incorporation of a high amount of RE ions and for fiber drawing, was selected for this research. The glass samples were synthesized by conventional melt-quenching method using chemicals with high purity level (99+%).

Three different glasses, named for short YE1 ÷ YE3, were obtained by doping the host material with a fixed level of Er_2O_3 (0.75 mol%) and an increasing level of Yb_2O_3 (ranging from 1.50 to 4.50 mol%) (see Table 2).

Table 2. Yb/Er co-doped phosphate glass compositions constituting the core of the optical amplifiers.

Glass name	Er^{3+} [10^{20} ions/cm^3]	Yb^{3+} [10^{20} ions/cm^3]
YE1	1.93	3.86
YE2	1.92	7.69
YE3	1.92	11.50

The fabricated glasses were cut and optically polished to 1 mm-thick samples for subsequent characterization. First of all, they were thermo-mechanically characterized, then the glasses underwent optical characterization such as refractive index measurement, Fourier-Transform Infrared (FTIR) spectroscopy and RE emission spectroscopy resolved in time and frequency. In parallel, the study of suitable cladding glass compositions for the core material was carried out and led to the synthesis of five glass compositions with tunable refractive index.

Single-material rod waveguides were then fabricated starting from the developed phosphate glasses YE1, YE2 and YE3, and using a custom induction heated optical fiber drawing tower. The rods feature a diameter of about 1 mm (see Fig. 2a).

A multi-mode optical fiber was also realized by preform drawing, with the fiber preform being obtained by the rod-in-tube technique, using the glass composition YE1 for the core and one of the developed cladding glass compositions for the cladding, with a targeted Numerical Aperture (NA) of 0.11. The optical fiber was fabricated in three different dimensions

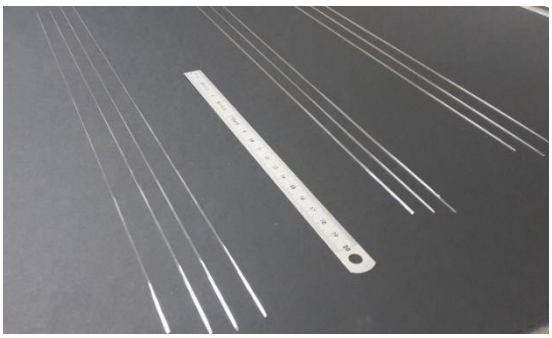

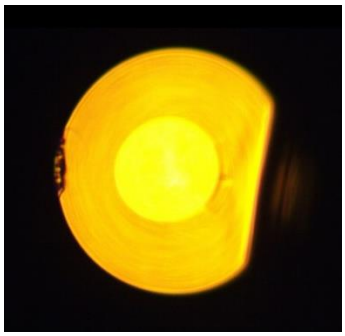

(core/cladding diameters): 50/125, 78/195, and 100/250 µm.

Figure 2. Optical amplifier waveguides: a) single-material rods, b) optical microscopy image of the multi-mode fiber.

The quality and morphology of the fabricated optical waveguides were inspected by means of an optical microscope. The cross-section of the multi-mode phosphate glass fiber is shown in Fig. 2b.

In order to assess the guiding properties of the fiber, a set of near-field images of the fiber cross-section was measured on a 120 cm-long fiber piece, at the wavelength of 1300 nm, using an end-face coupled fiber pigtailed laser diode source. The light was found well confined in the core.

Fiber losses were measured by the cut-back technique using a fiber length of about 120 cm with a single-mode fiber pigtailed laser diode source at 1300 nm. The attenuation value, as evaluated through a linear least

square fitting of the experimental data, was 3.6 dB/m. This value is mainly due to absorption and scattering effects.

The waveguides are currently under testing for amplification using a setup schematically shown in Fig. 3a. The initial seed employed was a Continuous Wave (CW) single-mode laser diode (center wavelength of 1548 nm) with an input of 36.5 mW. This seed was connected with a multi-mode pump laser (center wavelength of 912 nm) by means of a pump combiner. The output of the pump combiner (9/125 μm) was butt-coupled to the Er:Yb phosphate glass fiber with a 3-axis precision stage. A counter propagating second pump laser (976 nm with a core of 105 μm) was collimated with a 20 mm aspheric lens (L1), then propagated through a dichroic mirror and focused into the Er:Yb fiber cladding with a second 20 mm aspheric lens (L2). The amplified seed was reflected by the dichroic mirror and through an optical filter into the power meter. The first pump laser (pump 1 in Fig. 3a) was limited to 5.5 W, while the second pump laser (pump 2 in Fig. 3a) was limited to 3.5 W.

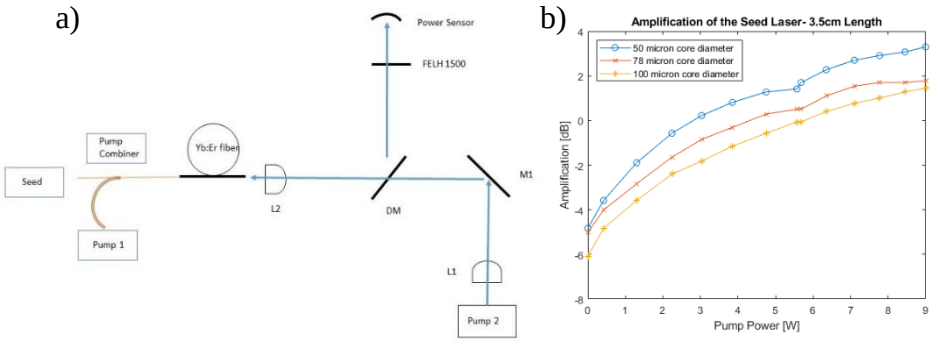

Figure 3. a) Setup used for the Er:Yb phosphate fiber amplification experiments. L1 and L2 are aspheric lens, DM is a dichroic mirror which transmits the 976 nm pump and reflects the 1548 nm of the seed, and FELH 1500 is a ThorLabs longpass filter. b) Seed output power as a function of the total power of pump laser diodes.

The initial experiments, performed with ~10 cm-long Er:Yb phosphate fibers, showed no amplification. During the experiments, it was observed that the seed amplification increased as the fiber core decreased. Very low amplification was obtained with the 100 μm fiber, while the amplification increased while using the 50 μm fiber. In addition, as the fiber length was shortened down to 3-4 cm, the amplification also enhanced.

The best result achieved up to now is reported in Fig. 3b. It was obtained with a 3.5 cm-long section of the 50 μm fiber. This result is equivalent to an amplification of 3.62 dB. It is worthwhile noting that the coupling and propagation losses of the seed in the active fiber were not taken into account, hence the actual amplification is underestimated.

The above reported are very preliminary amplification results with a low power CW seed. The enhancement of the amplification while decreasing the core diameter and the fiber length can be ascribed to the Amplified Spontaneous Emission (ASE) phenomenon. When the seed power is too low, the ASE in the amplifier depletes the gain, and consequently the amplification is low. This is also correlated to the core diameter. With larger diameters, the seed power has to be higher in order to saturate the amplifier and avoid the ASE effects. In addition, it is important to note that a large part of the pump power was not absorbed in the fiber because of its short length (cladding pumping).

Currently, fibers with smaller diameters are being fabricated and different doping concentrations will also be tested. Once satisfactory amplification will be obtained with these fibers, a pulsed microchip seed source will be employed and the amplification will be characterized.

4. The LIDAR system

A TOF LIDAR is a system which detects the time a light pulse takes to reach a target and propagate back to the receiver, allowing for the calculation of the distance to the target.

The main goal of the distance measurement is to create a 3D map of the surface. Scanning of an area is achieved by a rotating mirror or a prism, which is synchronized with the laser pulses, allowing for the generation of a 3D map.

Most LIDAR systems exploit a laser source due to its ability to focus high peak powers at relatively long distances. Typically, the laser is pulsed with a repetition rate that varies from few Hz to MHz (McCarthy et al., 2013; M. Ren et al., 2011; Budei at al., 2018). While using a high repetition rate in the order of the kHz, the pulse energy is relatively low (~1 nJ), but the peak power is still high (M. Ren et al., 2011; Spinhirne, 1993). The high peak power enabled operation at long distances.

In order to validate the range finding capability of the developed source, a laboratory setup was built with the aim to be used once the optimal parameters of the amplifier will be found (see Fig. 4a). The setup consists of a microchip Q-switched seed prototype, with a pulse width of ~2 ns, which is collimated with an aspheric lens and divided into two beams with a 10-90% beam splitter. The beam with 10% of the power is reflected with a mirror into the receiver, the second beam which is more powerful is sent to the target (a mirror up to now), and the reflected power is collected with a 2-inch diameter aspheric lens into the receiver.

Fig. 4b represents the two pulses which were detected with the receiver. One can observe that the time difference between the two peaks is 4.08 ns, which is equivalent to 1.23 meters, thus indicating that the distance between

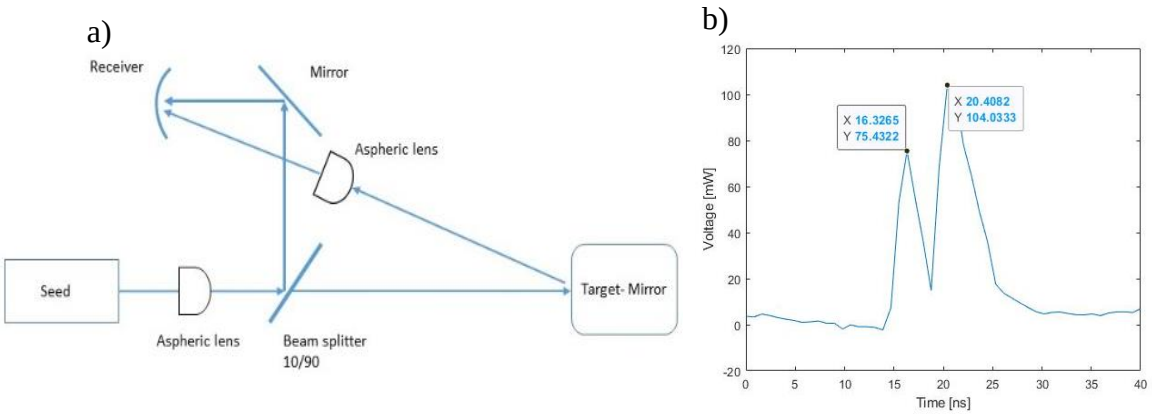

Figure 4. a) Laboratory setup used for distance measurements. b) Distance measurement performed with the home-made laboratory setup.

the beam splitter and the mirror was 61.2 cm. The actual distance was measured to be ~60 cm, corresponding to an error of 1.2 cm. This small error might also be associated to the length measurement of the two optical paths. As clearly visible from Fig. 4b, the difference between the two peaks can be determined with sub-ns resolution.

References

Boetti, N. G., Pugliese, D., Ceci-Ginistrelli, E., Lousteau, J., Janner, D., Milanese, D., 2017, Highly doped phosphate glass fibers for compact lasers and amplifiers: a review, *Appl. Sci.* **7**:1295.

Boetti, N. G., Scarpignato, G. C., Lousteau, J., Pugliese, D., Bastard, L., Broquin, J. -E., Milanese, D., 2015, High concentration Yb-Er co-doped phosphate glass for optical fiber amplification, *J. Opt.* **17**:065705.

Budei, B. C., St-Onge, B., Hopkinson, C., Audet, F.-A., 2018, Identifying the genus or species of individual trees using a three-wavelength airborne lidar system, *Remote Sens. Environ.* **204**:632-647.

Chen, M., Rudd, W. J., Hansell, J., Pachowicz, D., Litvinovitch, S., Burns, P., Sawruk, N. W., 2019, Er:YAG methane lidar laser technology, Proc. SPIE 11005, Laser Radar Technology and Applications XXIV, 110050Q.

Gorbachenya, K. N., Kisel, V. E., Yasukevich, A. S., Maltsev, V. V., Leonyuk, N. I., Kuleshov, N. V., 2015, CW and Q-switched diode-pumped laser operation of Er,Yb:$GdAl_3(BO_3)_4$ crystal, Advanced Solid State Lasers (ASSL) 2015, Berlin, Germany, paper ATu1A.5.

Häring, R., Paschotta, R., Fluck, R., Gini, E., Melchior, H., Keller, U., 2001, Passively Q-switched microchip laser at 1.5 μm, *J. Opt. Soc. Am. B: Opt. Phys.* **18**:1805-1812.

https://esto.nasa.gov/files/Lidar_TechStrategy_%202016.pdf

https://www.nato.int/cps/en/natohq/85291.htm

Jiang, S., Mendes, S. B., Hu, Y., Nunzi-Conti, G., Chavez-Pirson, A., Kaneda, Y., Luo, T., Chen, Q., Hocde, S., Nguyen, D. T., Wright, E. M., Wang, J., Tian, W., Nikolajsen, T., Peyghambarian, N., 2003, Compact multimode pumped erbium-doped phosphate fiber amplifiers, *Opt. Eng.* **42**:2817-2820.

Lee, Y. -W., Sinha, S., Digonnet, M. J. F., Byer, R. L., Jiang, S., 2006, 20 W single-mode Yb^{3+}-doped phosphate fiber laser, *Opt. Lett.* **31**:3255-3257.

McCarthy, A., Ren, X., Della Frera, A., Gemmell, N. R., Krichel, N. J., Scarcella, C., Ruggeri, A., Tosi, A., Buller G. S., 2013, Kilometer-range depth imaging at 1550 nm wavelength using an InGaAs/InP single-photon avalanche diode detector, *Opt. Express* **21**:22098-22113.

Overton, G., 2017, Lasers for Lidar: Application parameters dictate laser source selection in lidar systems, LaserFocusWorld.

Pulikkaseril, C., and Lam, S., 2019, Laser eyes for driverless cars: the road to automotive LIDAR, Optical Fiber Communication Conference (OFC) 2019, San Diego, USA, paper Tu3D.2.

Qiu, T., Li, L., Schülzgen, A., Temyanko, V. L., Luo, T., Jiang, S., Mafi, A., Moloney, J. V., Peyghambarian, N., 2004, Generation of 9.3-W multimode and 4-W single-mode output from 7-cm short fiber lasers, *IEEE Photonics Technol. Lett.* **16**:2592-2594.

Ren, M., Gu, X., Liang, Y., Kong, W., Wu, E., Wu, G., Zeng, H., 2011, Laser ranging at 1550 nm with 1-GHz sine-wave gated InGaAs/InP APD single-photon detector, *Opt. Express* **19**:13497-13502.

Schmitt, N. P., 2017, Research results, lessons learned and future perspective of forward-looking LIDAR for aircraft, 2017 Conference on Lasers and Electro-Optics (CLEO), San Jose, USA, pp. 1–2.

Spinhirne, J. D., 1993, Micro pulse lidar, *IEEE Trans. Geosci. Remote Sens.* **31**:48-55.

Spinhirne, J. D., Rall, J. A. R., Scott, V. S., 1995, Compact eye safe Lidar systems, *Rev. Laser Eng.* **23**:112-118.

Yamane, M., and Asahara, Y., 2004, *Glasses for Photonics*, Cambridge University Press, Cambridge.

Zayhowski, J. J., 2013, Microchip Lasers, in: *Handbook of Solid-State Lasers: Materials, Systems and Applications*, B. Denker and E. Shklovsky, eds., Woodhead Publishing, Cambridge, U.K., pp. 359-402.